

Reissner's Mixed Variational Theorem toward MITC finite elements for multilayered plates.

Original

Reissner's Mixed Variational Theorem toward MITC finite elements for multilayered plates / Chinosi, C.; Cinefra, Maria; Della Croce, L.; Carrera, Erasmo. - In: COMPOSITE STRUCTURES. - ISSN 0263-8223. - 99:(2013), pp. 443-452. [10.1016/j.compstruct.2012.11.007]

Availability:

This version is available at: 11583/2503876 since:

Publisher:

A.J.M. Ferreira

Published

DOI:10.1016/j.compstruct.2012.11.007

Terms of use:

This article is made available under terms and conditions as specified in the corresponding bibliographic description in the repository

Publisher copyright

(Article begins on next page)

Reissner's Mixed Variational Theorem toward MITC finite elements for multilayered plates

Claudia Chinosi^a, Maria Cinefra^b, Lucia Della Croce^c, Erasmo Carrera^{b,*}

^a*Department of Sciences and Technological Innovation, Università del Piemonte Orientale, Alessandria, Italy*

^b*Aerospace Engineering Department, Politecnico di Torino, Torino, Italy*

^c*Department of Mathematics, Università di Pavia, Pavia, Italy*

Abstract

In this paper, we analyze a two dimensional model of multilayered plates for which the main interest is to study the mechanical response, that may change in the thickness direction. The finite element method showed successful performances to approximate the solutions of the advanced structures. In this regard, two variational formulations are available to reach the stiffness matrices, the principle of virtual displacement (PVD) and the Reissner mixed variational theorem (RMVT). Here we introduce a strategy similar to MITC (Mixed Interpolated of Tensorial Components) approach, in the RMVT formulation, in order to construct an advanced locking-free finite element. Assuming the transverse stresses as independent variables, the continuity at the interfaces between layers is easily imposed. It is known that unless the combination of finite element spaces for displacement and stresses is chosen carefully, the problem of locking is likely to occur. Following this suggestion, we propose a finite element scheme that it is known to be robust with respect to the locking phenomenon in the classical PVD approach. We show that in the RMVT context, the element exhibits both properties of convergence and robustness when comparing the numerical results with benchmark solutions from literature.

Key words: Multilayered plate, Finite Elements, Mixed Interpolation of Tensorial Components, Reissner Mixed Variational Theorem;

1. Introduction

Multilayered structures are increasingly used in many fields. Examples of multilayered, anisotropic structures are sandwich constructions, composite structures made of orthotropic laminae or layered structures made of different isotropic layers (such as those employed for thermal protection). In most of the applications, these structures mostly appear as flat (plates) or curved panels (shells). In this paper, attention has been restricted to flat structures made of different isotropic layers, although the models could be easily extended to other cases.

The analysis of multilayered structures is difficult

when compared to one layered ones. A number of complicating effects arise when their mechanical behavior as well as failure mechanisms have to be correctly understood. This is due to the intrinsic discontinuity of the mechanical properties at each layer–interface to which high shear and normal transverse deformability is associated. An accurate description of the stress and strain fields of these structures requires theories that are able to satisfy the so-called Interlaminar Continuity (IC) conditions for the transverse stresses (see Whitney [1], and Pagano [2], as examples). Transverse anisotropy of multilayered structures make it difficult to find closed form solutions and the use of approximated solutions is necessary. It can therefore be concluded that the use of both refined two-dimensional theories and computational methods become mandatory to solve practical problems re-

*Corresponding author.

Email addresses: erasmo.carrera@polito.it (Erasmo Carrera)

Preprint submitted to Composite Structures

October 12, 2012

lated to multilayered structures.

Among the several available computational methods, the Finite Element Method (FEM) has played and continues to play a significant role. In this work, the Reissner's Variational Mixed Theorem (RMVT) is used to derive plate finite elements. As a main property, RMVT permits one to assume two independent fields for displacement and transverse stress variables. The resulting advanced finite elements therefore describe *a priori* interlaminar continuous transverse stress fields.

For a complete and rigorous understanding of the foundations of RMVT, reference can be made to the articles by Professor Reissner [3]-[5] and the review article by Carrera [6]. The first application of RMVT to modeling of multilayered flat structures was performed by Murakami [7],[8]. He introduced a first order displacement field in his papers, in conjunction with an independent parabolic transverse stress LW field in each layer (transverse normal stress and strain were discarded). An extension to a higher order displacement field was proposed by Toledano and Murakami in [9]. While in [10], they extended the RMVT to a layer-wise description of both displacement and transverse stress fields. These papers [7]-[10] should be considered as the fundamental works in the applications of RMVT as a tool to model multilayered structures. Further discussions on RMVT were provided by Soldatos [11]. A generalization, proposing a systematic use of RMVT as a tool to furnish a class of two dimensional theories for multilayered plate analysis, was presented by Carrera [12]-[14]. The order of displacement fields in the layer was taken as a free parameter of the theories. Applications of what is reported in [12],[13] have been given in several other papers [15]-[22], in which closed-form solution are considered. Layer-wise mixed analyses were performed in [23] for the static case. As a fundamental result, the numerical analysis demonstrated that RMVT furnishes a quasi three-dimensional a priori description of transverse stresses, including transverse normal components. Sandwich plates were also considered in [16]. Recently, Messina [24] has compared RMVT results to PVD (Principle of Virtual Displacements) ones. Transverse normal stresses were, however, discarded in this work. In [25]-[27], Carrera and Demasi developed multilayered plate elements based on RMVT, that were able to give a quasi-three-dimensional description of stress/strain fields. But in these works, they

still employ the selective reduced integration [28] to overcome the shear locking phenomenon.

Recently, authors adopted the Mixed Interpolation of Tensorial Components (MITC) to contrast the locking. According to this technique, the strain components are not directly computed from the displacements but they are interpolated within each element using a specific interpolation strategy for each component. For more details about MITC, the readers can refer to the works [29]-[33]. In [34], the authors formulated plate/shell elements based on displacement formulation that showed good properties of convergence thanks to the use of the MITC. The idea of this work is to interpolate the transverse stresses (that are modelled a-priori by the RMVT) using the same strategy of the MITC. In this way, the RMVT permits both to satisfy IC conditions and to withstand the shear locking.

The plate elements here proposed have nine nodes. The displacement field is defined according to the Reissner-Mindlin theory and the shear stresses are assumed parabolic along the thickness by means of RMVT. The normal strain ϵ_{zz} and the normal stress σ_{zz} are discarded. The shear stresses σ_{xz} and σ_{yz} are interpolated in each element according to the MITC. Plate finite elements based on Reissner-Mindlin assumptions, but formulated in the framework of RMVT (shear stresses are modelled a-priori), are considered for comparison purposes. Comparisons with 3D solutions are also provided. Future companion works will be devoted to the analysis of multilayered shell structures and the extension to higher-order models.

2. Reissner Mixed Variational Theorem (RMVT)

The stress vector $\boldsymbol{\sigma} = (\sigma_i)$, $i = 1, \dots, 6$ can be written in terms of the in-plane and transverse components as $\boldsymbol{\sigma} = [\boldsymbol{\sigma}_p \ \boldsymbol{\sigma}_n]$ with:

$$\boldsymbol{\sigma}_p = [\sigma_{xx} \ \sigma_{yy} \ \sigma_{xy}]^T, \quad \boldsymbol{\sigma}_n = [\sigma_{xz} \ \sigma_{yz} \ \sigma_{zz}]^T \quad (1)$$

and analogously the strain vector $\boldsymbol{\epsilon} = (\epsilon_i)$, $i = 1, \dots, 6$ can be written in terms of the in-plane and transverse components as $\boldsymbol{\epsilon} = [\boldsymbol{\epsilon}_p \ \boldsymbol{\epsilon}_n]$, with:

$$\boldsymbol{\epsilon}_p = [\epsilon_{xx} \ \epsilon_{yy} \ \epsilon_{xy}]^T, \quad \boldsymbol{\epsilon}_n = [\epsilon_{xz} \ \epsilon_{yz} \ \epsilon_{zz}]^T \quad (2)$$

The PVD variational equation is written as:

$$\int_V (\delta \epsilon_{pG}^T \sigma_{pH} + \delta \epsilon_{nG}^T \sigma_{nH}) dV = \delta L_e \quad (3)$$

The subscript H means that the stresses are computed by Hooke's law, while the subscript G means that the strains are computed from geometrical relations. The superscript T stands for transposition operation, V represents the 3D multilayered body volume. δL_e is the virtual variation of the work.

In the RMVT formulation the transverse stresses are assumed as independent variables and denoted by σ_{nM} (M stands for *Model*). The transverse strains are evaluated by Hooke's law and denoted by ϵ_{nH} . They should be related to the geometrical strains ϵ_{nG} by the constraint equation:

$$\epsilon_{nH} = \epsilon_{nG}. \quad (4)$$

By adding in (3) the compatibility condition (4) through a Lagrange multipliers field, which turn out to be transverse stresses, one then obtain the RMVT formulation:

$$\begin{aligned} \int_V (\delta \epsilon_{pG} \sigma_{pH} + \delta \epsilon_{nG} \sigma_{nM} + \delta \sigma_{nM} (\epsilon_{nG} - \epsilon_{nH})) dV \\ = \delta L_e \end{aligned} \quad (5)$$

The third 'mixed' term variationally enforces the compatibility of the transverse strain components.

2.1. The constitutive equations and the geometrical relations

In this section we will explain in detail the construction of RMVT employing the Hooke's law and the geometrical relations (see for example [26]).

Referring to the Hooke's law for orthotropic material $\sigma_i = \tilde{C}_{ij} \epsilon_j$, $i, j = 1, \dots, 6$ the constitutive equations become:

$$\begin{aligned} \sigma_{pH} &= \tilde{C}_{pp} \epsilon_{pG} + \tilde{C}_{pn} \epsilon_{nG} \\ \sigma_{nH} &= \tilde{C}_{np} \epsilon_{pG} + \tilde{C}_{nn} \epsilon_{nG} \end{aligned} \quad (6)$$

where the material matrices are:

$$\begin{aligned} \tilde{C}_{pp} &= \begin{bmatrix} \tilde{C}_{11} & \tilde{C}_{12} & \tilde{C}_{16} \\ \tilde{C}_{12} & \tilde{C}_{22} & \tilde{C}_{26} \\ \tilde{C}_{16} & \tilde{C}_{26} & \tilde{C}_{66} \end{bmatrix} \quad \tilde{C}_{pn} = \begin{bmatrix} 0 & 0 & \tilde{C}_{13} \\ 0 & 0 & \tilde{C}_{23} \\ 0 & 0 & \tilde{C}_{36} \end{bmatrix} \\ \tilde{C}_{np} &= \tilde{C}_{pn}^T; \quad \tilde{C}_{nn} = \begin{bmatrix} \tilde{C}_{44} & \tilde{C}_{45} & 0 \\ \tilde{C}_{45} & \tilde{C}_{55} & 0 \\ 0 & 0 & \tilde{C}_{33} \end{bmatrix} \end{aligned} \quad (7)$$

From the second equation of (6) we obtain

$$\epsilon_{nG} = -(\tilde{C}_{nn})^{-1} \tilde{C}_{np} \epsilon_{pG} + (\tilde{C}_{nn})^{-1} \sigma_{nH} \quad (8)$$

We note that the right side of the above relation can be assumed as definition of transverse strains from Hooke's law, ϵ_{nH} .

After substitution into the first equation of (6) we obtain:

$$\begin{aligned} \sigma_{pH} &= [\tilde{C}_{pp} - \tilde{C}_{pn} (\tilde{C}_{nn})^{-1} \tilde{C}_{np}] \epsilon_{pG} + \\ &\quad \tilde{C}_{pn} (\tilde{C}_{nn})^{-1} \sigma_{nH}. \end{aligned} \quad (9)$$

The transverse stresses σ_{nH} appearing in (8) and (9) represent the independent variables of our model which are thus indicated by σ_{nM} . The equation (8) together with (9) lead to the mixed form of Hooke's law.

$$\begin{aligned} \sigma_{pH} &= C_{pp} \epsilon_{pG} + C_{pn} \sigma_{nM} \\ \epsilon_{nH} &= C_{np} \epsilon_{pG} + C_{nn} \sigma_{nM} \end{aligned} \quad (10)$$

where

$$\begin{aligned} C_{pp} &= [\tilde{C}_{pp} - \tilde{C}_{pn} (\tilde{C}_{nn})^{-1} \tilde{C}_{np}] \\ C_{pn} &= \tilde{C}_{pn} (\tilde{C}_{nn})^{-1} \\ C_{np} &= -(\tilde{C}_{nn})^{-1} \tilde{C}_{np} \\ C_{nn} &= (\tilde{C}_{nn})^{-1} \end{aligned} \quad (11)$$

As regards the geometrical relations defining the strains, we assume the hypothesis of small deformation field. In this case the in-plane and transverse strains are related to displacements $\mathbf{u} = [u_x \ u_y \ u_z]$ through the linear differential relations:

$$\epsilon_{pG} = \mathbf{D}_p \mathbf{u} = \begin{bmatrix} \partial x & 0 & 0 \\ 0 & \partial y & 0 \\ \partial x & \partial y & 0 \end{bmatrix} \begin{bmatrix} u_x \\ u_y \\ u_z \end{bmatrix} \quad (12)$$

and

$$\epsilon_{nG} = \mathbf{D}_z \mathbf{u} = \begin{bmatrix} \partial z & 0 & \partial x \\ 0 & \partial z & \partial y \\ 0 & 0 & \partial z \end{bmatrix} \begin{bmatrix} u_x \\ u_y \\ u_z \end{bmatrix} \quad (13)$$

In RMVT the compatibility condition of the transverse strains is enforced by equating the second equation of (10) with (13).

3. The First Order Shear Deformation Theory (FSDT) for plates

The plate theory suggested by Reissner [36] and Mindlin [37] takes into account the transverse shear deformations. The theory, also known as FSDT, uses the assumption that particles of the plate originally on a line that is normal to the undeformed middle surface remain on a straight line during deformation, but this line is not necessarily normal to the deformed middle surface. It assumes the following kinematic assumptions:

$$\begin{aligned} u_x(x, y, z) &= z \theta_x(x, y) \\ u_y(x, y, z) &= z \theta_y(x, y) \\ u_z(x, y, z) &= w(x, y) \end{aligned} \quad (14)$$

The functions θ_x and θ_y are the rotations of the normal to the undeformed middle surface in the x - z and y - z planes, respectively. We observe that both the transverse displacement and the rotations depend only on (x, y) .

3.1. FSDT in the PVD formulation

The PVD formulation (3) using (6), (12), (13) becomes

$$\begin{aligned} \int_V \left[(\mathbf{D}_p \delta \mathbf{u})^T (\tilde{\mathbf{C}}_{pp} \mathbf{D}_p \mathbf{u} + \tilde{\mathbf{C}}_{pn} \mathbf{D}_z \mathbf{u}) + \right. \\ \left. (\mathbf{D}_z \delta \mathbf{u})^T (\tilde{\mathbf{C}}_{np} \mathbf{D}_p \mathbf{u} + \tilde{\mathbf{C}}_{nn} \mathbf{D}_z \mathbf{u}) \right] dV = \delta L_e \end{aligned} \quad (15)$$

The Reissner-Mindlin assumptions lead to write

$$\begin{aligned} \mathbf{D}_p \mathbf{u} &= \left[z \frac{\partial \theta_x}{\partial x}, \quad z \frac{\partial \theta_y}{\partial y}, \quad z \left(\frac{\partial \theta_x}{\partial y} + \frac{\partial \theta_y}{\partial x} \right) \right]^T \\ \mathbf{D}_z \mathbf{u} &= \left[\theta_x + \frac{\partial w}{\partial x}, \quad \theta_y + \frac{\partial w}{\partial y}, \quad 0 \right]^T. \end{aligned} \quad (16)$$

We observe that the Mindlin hypothesis $\sigma_{zz} = 0$ decouples the in-plane and out-of-plane stress and strain components. Thus the constitutive relations can be written as in (6) with both $\tilde{\mathbf{C}}_{pn}$ and $\tilde{\mathbf{C}}_{np}$ null matrices. The other material matrices can be expressed in terms of the Young's modulus of elasticity E and the Poisson's ratio ν in the following way:

$$\tilde{\mathbf{C}}_{pp} = \frac{E}{1 - \nu^2} \begin{bmatrix} 1 & \nu & 0 \\ \nu & 1 & 0 \\ 0 & 0 & \frac{1-\nu}{2} \end{bmatrix} \quad (17)$$

$$\tilde{\mathbf{C}}_{nn} = \frac{E}{2(1 + \nu)} \begin{bmatrix} 1 & 0 & 0 \\ 0 & 1 & 0 \\ 0 & 0 & 0 \end{bmatrix} \quad (18)$$

The FSDT connected to the PVD formulation produce the following variational statement

$$\int_V \left[(\mathbf{D}_p \delta \mathbf{u})^T \tilde{\mathbf{C}}_{pp} \mathbf{D}_p \mathbf{u} + (\mathbf{D}_z \delta \mathbf{u})^T \tilde{\mathbf{C}}_{nn} \mathbf{D}_z \mathbf{u} \right] dV = \delta L_e \quad (19)$$

Let us suppose that the plate occupies, in absence of forces, a region $V = \Omega \times (-\frac{t}{2}, \frac{t}{2})$, where Ω is a bounded smooth domain with boundary $\partial\Omega$ and $t > 0$ is the thickness of the plate which is assumed small with respect to $\text{diam}(\Omega)$. The plate is subjected to a vertical load $\mathbf{p} = (0, 0, p(x, y))$ acting in z direction.

Let $\boldsymbol{\kappa}(\boldsymbol{\theta})$ be the three-component vector of curvatures

$$\boldsymbol{\kappa}(\boldsymbol{\theta}) = \left[\frac{\partial \theta_x}{\partial x}, \quad \frac{\partial \theta_y}{\partial y}, \quad \frac{\partial \theta_x}{\partial y} + \frac{\partial \theta_y}{\partial x} \right]^T, \quad \boldsymbol{\theta} = [\theta_x, \theta_y]^T \quad (20)$$

let $\boldsymbol{\gamma}(\boldsymbol{\theta}, w)$ be the reduced two-components vector of transverse shear strains

$$\boldsymbol{\gamma}(\boldsymbol{\theta}, w) = \left[\theta_x + \frac{\partial w}{\partial x}, \quad \theta_y + \frac{\partial w}{\partial y} \right]^T, \quad (21)$$

let $\bar{\mathbf{C}}_{nn}$ be the 2×2 reduced matrix

$$\bar{\mathbf{C}}_{nn} = \frac{E}{2(1 + \nu)} \mathbf{I}_2 \quad (22)$$

and \mathbf{I}_2 the 2×2 identity matrix.

Integrating (19) along the thickness, the variational formulation of Reissner-Mindlin plate problem is to find $(\boldsymbol{\theta}, w)$ such that:

$$\begin{aligned} \frac{t^3}{12} \int_{\Omega} (\delta \boldsymbol{\kappa}(\boldsymbol{\theta}))^T \tilde{\mathbf{C}}_{pp} \boldsymbol{\kappa}(\boldsymbol{\theta}) d\Omega + \\ tk \int_{\Omega} (\delta \boldsymbol{\gamma}(\boldsymbol{\theta}, w))^T \bar{\mathbf{C}}_{nn} \boldsymbol{\gamma}(\boldsymbol{\theta}, w) d\Omega = t \int_{\Omega} \delta w p(x, y) d\Omega \end{aligned} \quad (23)$$

The constant k appearing in (23) contains shear correction factors to account for the non-uniformity of the transverse shear stresses through the plate thickness.

3.2. FSDT in the RMVT formulation

In the framework of RMVT we replace in (5) the relations (10). The use of (12) and (13) lead to the following formulation in terms of the independent variables \mathbf{u} and $\boldsymbol{\sigma}_{nM}$:

$$\int_V [(\mathbf{D}_p \delta \mathbf{u})^T (\mathbf{C}_{pp} \mathbf{D}_p \mathbf{u} + \mathbf{C}_{pn} \boldsymbol{\sigma}_{nM}) + (\mathbf{D}_z \delta \mathbf{u})^T \boldsymbol{\sigma}_{nM} + (\delta \boldsymbol{\sigma}_{nM})^T (\mathbf{D}_z \mathbf{u} - \mathbf{C}_{np} \mathbf{D}_p \mathbf{u} - \mathbf{C}_{nn} \boldsymbol{\sigma}_{nM})] dV = \delta L_e \quad (24)$$

The plain stress assumption of the Reissner-Mindlin theory ($\sigma_{zz} = 0$) implies that the transverse stress vector is reduced to a two components vector:

$$\boldsymbol{\sigma}_{nM} = [\sigma_{xz} \ \sigma_{yz}]$$

and, as above, the mixed form of Hooke's law can be written as in (10) with both \mathbf{C}_{pn} and \mathbf{C}_{np} null matrices and

$$\begin{aligned} \mathbf{C}_{pp} &= \tilde{\mathbf{C}}_{pp} \\ \mathbf{C}_{nn} &= (\tilde{\mathbf{C}}_{nn})^{-1} = \frac{2(1+\nu)}{E} \mathbf{I}_2 \end{aligned} \quad (25)$$

In matricial form the Reissner-Mindlin formulation in RMVT context states:

$$\begin{aligned} \int_V \begin{bmatrix} (\mathbf{D}_p \delta \mathbf{u})^T \mathbf{C}_{pp} \mathbf{D}_p & (\bar{\mathbf{D}}_z \delta \mathbf{u})^T \\ (\delta \boldsymbol{\sigma}_{nM})^T \bar{\mathbf{D}}_z & -(\delta \boldsymbol{\sigma}_{nM})^T \mathbf{C}_{nn} \end{bmatrix} \begin{bmatrix} \mathbf{u} \\ \boldsymbol{\sigma}_{nM} \end{bmatrix} dV \\ = \int_V \begin{bmatrix} (\delta \mathbf{u})^T \mathbf{p} \\ \mathbf{0} \end{bmatrix} dV \end{aligned} \quad (26)$$

where $\bar{\mathbf{D}}_z$ is the 2×3 reduced differential operator:

$$\bar{\mathbf{D}}_z = \begin{bmatrix} \partial z & 0 & \partial x \\ 0 & \partial z & \partial y \end{bmatrix} \quad (27)$$

Integrating (26) along the thickness, the problem is to find $(\boldsymbol{\theta}, w, \boldsymbol{\sigma}_{nM})$ such that:

$$\begin{cases} \frac{t^3}{12} \int_{\Omega} (\delta \boldsymbol{\kappa}(\boldsymbol{\theta}))^T \mathbf{C}_{pp} \boldsymbol{\kappa}(\boldsymbol{\theta}) d\Omega + \\ tk \int_{\Omega} (\delta \boldsymbol{\gamma}(\boldsymbol{\theta}, w))^T \boldsymbol{\sigma}_{nM} d\Omega = t \int_{\Omega} \delta w p(x, y) d\Omega \\ tk \int_{\Omega} (\delta \boldsymbol{\sigma}_{nM})^T \boldsymbol{\gamma}(\boldsymbol{\theta}, w) d\Omega - \\ t \int_{\Omega} (\delta \boldsymbol{\sigma}_{nM})^T \mathbf{C}_{nn} \boldsymbol{\sigma}_{nM} dx dy = 0 \end{cases} \quad (28)$$

In order to approximate the problem (28) by finite element method we introduce the suitable spaces: $\boldsymbol{\Theta}$, W and $\boldsymbol{\Sigma}$ of admissible rotations, vertical displacement and transverse stresses respectively. We can state the related mixed problem in this way:

$$\begin{cases} \text{Find } (\boldsymbol{\theta}, w, \boldsymbol{\sigma}) \in \boldsymbol{\Theta} \times W \times \boldsymbol{\Sigma} : \\ \frac{t^3}{12} a(\boldsymbol{\eta}, \boldsymbol{\theta}) + tk(\boldsymbol{\eta} + \nabla v, \boldsymbol{\sigma}) = t(v, p) \\ \forall (\boldsymbol{\eta}, v) \in \boldsymbol{\Theta} \times W, \\ tk(\boldsymbol{\xi}, \boldsymbol{\theta} + \nabla w) - tk \frac{2(1+\nu)}{E} (\boldsymbol{\xi}, \boldsymbol{\sigma}) = 0 \quad \forall \boldsymbol{\xi} \in \boldsymbol{\Sigma}, \end{cases} \quad (29)$$

where $\boldsymbol{\sigma}$ stands for $\boldsymbol{\sigma}_{nM}$ and

$$a(\boldsymbol{\eta}, \boldsymbol{\theta}) := \int_{\Omega} (\boldsymbol{\kappa}(\boldsymbol{\eta}))^T \mathbf{C}_{pp} \boldsymbol{\kappa}(\boldsymbol{\theta}) d\Omega, \quad (30)$$

(\cdot, \cdot) is the inner-product in the space $L^2(\Omega)$ of square integrable functions in Ω .

4. EM1-2 model based on RMVT for multi-layered plates

In this work we adopt a mixed theory with equivalent single layer (**ESL**) descriptions for the displacements \mathbf{u} and a layerwise (**LW**) description for the transverse stresses $\boldsymbol{\sigma}$. In particular we use the first order expansion (14) of the Reissner-Mindlin model for the displacements field, while we assume that the transverse stresses are parabolic functions independent in each layer. Thus, referring to the usual notations, we denote our model by the code EM1-2. Let the multilayered structure occupies a region $V = \Omega \times (-\frac{t}{2}, \frac{t}{2})$, where Ω is a bounded smooth domain with boundary $\partial\Omega$ and $t > 0$ is the thickness of the structure, which is divided into a certain number of layers N_l , that are supposed to be perfectly bonded together. The multilayered constructions introduce further requirements respect to the one-layer plates made of isotropic materials. Actually for equilibrium reasons the transverse stresses are required to be continuous in each layer interface. Then the fulfilment of the interlaminar continuity (IC) is a crucial point of the two dimensional modelling of multilayered structures. To do this we use a suitable combination of Legendre polynomials as basis functions of the parabolic expansion for the transverse stresses $\boldsymbol{\sigma}_{nM} = [\sigma_{xz}, \sigma_{yz}]$. In any k -layer, $k = 1, \dots, N_l$ we assume:

$$\begin{aligned} \sigma_{xz} &= F_t(z) \sigma_{xz_t} + F_b(z) \sigma_{xz_b} + F_2(z) \sigma_{xz_2} \\ \sigma_{yz} &= F_t(z) \sigma_{yz_t} + F_b(z) \sigma_{yz_b} + F_2(z) \sigma_{yz_2} \end{aligned} \quad (31)$$

The subscripts t and b denote values related to the k -layer top and bottom surfaces respectively, z is the physical coordinate of the k -layer, $-t_k/2 \leq z \leq t_k/2$ and the thickness functions $F_t(z)$, $F_b(z)$, $F_2(z)$ are defined as follows:

$$\begin{aligned} F_t(z) &= \frac{P_0 + P_1}{2}, & F_b(z) &= \frac{P_0 - P_1}{2}, \\ F_2(z) &= P_2 - P_0, \end{aligned} \quad (32)$$

where $P_j = P_j(z)$ is the Legendre polynomial of j -order. By introducing the non-dimensional layer coordinate $\xi_k = 2z/t_k$, $-1 \leq \xi_k \leq 1$ the Legendre polynomials are:

$$P_0 = 1, \quad P_1 = \xi_k, \quad P_2 = \frac{3\xi_k^2 - 1}{2} \quad (33)$$

The interlaminar transverse stress continuity (IC) is linked by writing:

$$\begin{aligned} \sigma_{xz_t}^k &= \sigma_{xz_b}^{k+1} \\ \sigma_{yz_t}^k &= \sigma_{yz_b}^{k+1} \end{aligned} \quad (34)$$

for $k = 1, \dots, N_l - 1$. In each layer the unknowns are $(\boldsymbol{\theta}, w, \tilde{\boldsymbol{\sigma}})$, where the independent shear stress tensor $\tilde{\boldsymbol{\sigma}}$ is

$$\tilde{\boldsymbol{\sigma}} = [\boldsymbol{\sigma}_t, \boldsymbol{\sigma}_b, \boldsymbol{\sigma}_2] = \begin{bmatrix} \sigma_{xz_t} & \sigma_{xz_b} & \sigma_{xz_2} \\ \sigma_{yz_t} & \sigma_{yz_b} & \sigma_{yz_2} \end{bmatrix} \quad (35)$$

In the RMVT formulation for multilayered structures by using our EM1-2 approach, the problem (29) considered in each layer becomes as follows:

$$\left\{ \begin{array}{l} \text{Find } (\boldsymbol{\theta}, w, \tilde{\boldsymbol{\sigma}}) \in \boldsymbol{\Theta} \times W \times \Sigma^3 : \\ \frac{t^3}{12} a(\boldsymbol{\eta}, \boldsymbol{\theta}) + (\boldsymbol{\eta} + \nabla v, \tilde{\boldsymbol{\sigma}} \mathbf{c}) = t(v, p) \\ \quad \forall (\boldsymbol{\eta}, v) \in \boldsymbol{\Theta} \times W, \\ (c_t \boldsymbol{\xi}_t, \boldsymbol{\theta} + \nabla w) - \frac{2(1+\nu)}{E} (c_t \boldsymbol{\xi}_t, \tilde{\boldsymbol{\sigma}} \mathbf{c}) = 0 \quad \forall \boldsymbol{\xi}_t \in \Sigma, \\ (c_b \boldsymbol{\xi}_b, \boldsymbol{\theta} + \nabla w) - \frac{2(1+\nu)}{E} (c_b \boldsymbol{\xi}_b, \tilde{\boldsymbol{\sigma}} \mathbf{c}) = 0 \quad \forall \boldsymbol{\xi}_b \in \Sigma, \\ (c_2 \boldsymbol{\xi}_2, \boldsymbol{\theta} + \nabla w) - \frac{2(1+\nu)}{E} (c_2 \boldsymbol{\xi}_2, \tilde{\boldsymbol{\sigma}} \mathbf{c}) = 0 \quad \forall \boldsymbol{\xi}_2 \in \Sigma, \end{array} \right. \quad (36)$$

where

$$\mathbf{c} = [c_t, c_b, c_2] = \begin{bmatrix} \int_{-t_k/2}^{t_k/2} F_t(z) dz \\ \int_{-t_k/2}^{t_k/2} F_b(z) dz \\ \int_{-t_k/2}^{t_k/2} F_2(z) dz \end{bmatrix} \quad (37)$$

In Figure 1, the assembling of stiffness matrix at multilayer-level is shown. A plate structure made of 3 layer is considered. The stiffness matrices of the layers are summed where the ESL description is used (displacements) and the continuity conditions are imposed (shear stresses).

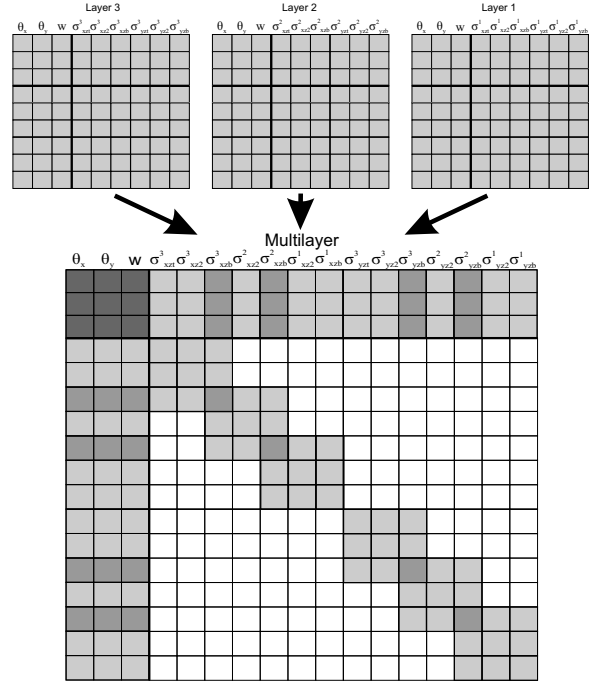


Figure 1: Assembling procedure of stiffness matrix.

5. Finite element approximation

The multilayered plate model (36) based on RMVT involves the Reissner-Mindlin plate system (29). Thus the finite element approximation of problem (36) can be related to the finite element techniques typically used for the plate. For this reason, we present at first the discretization of the plate problem (29) then we generalize in the case of multilayered plate.

5.1. MITC plate element

It is well known that the numerical approximation of the Reissner-Mindlin plate problem is not straightforward. When standard finite element methods are applied to the classical transversal displacement-rotations formulation of the plate the

solution degenerates very rapidly for small thickness (*locking* phenomenon). To overcome such a behavior a mixed interpolation techniques are usually adopted to weaken or possibly eliminate the shear locking of the numerical solution. In this regard, generalizing the basic idea of Bathe and Dvorkin ([38]), using a non standard formulation Brezzi *et al.* ([30]) have introduced mixed–interpolated finite elements (MITC) and have given a mathematical analysis proving the stability of the elements. The chief idea is to reduce the effect of the shear term by choosing carefully the combination of the finite element spaces for displacement and shear stresses. In this paper, we introduce a strategy similar to MITC approach tailored to the RMVT formulation in order to construct an advanced locking-free finite element to treat the multilayered plates. In this paper we consider a particular MITC finite element, known as MITC9 (see [39]).

Let we introduce a shape regular and conforming quadrilateral grid \mathcal{T}_h of elements of diameter h for the domain Ω , which we assume polygonal for simplicity. The MITC9 element is characterized by the following choice of the finite element spaces $\Theta_h = \Theta_h \times \Theta_h$, W_h , Σ_h has been carried out:

$$\Theta_h = \{v \in H^1(\Omega) : v|_E \in Q_2(E) \ \forall E \in \mathcal{T}_h\} \quad (38)$$

where $Q_2(E)$ is the space of polynomials of degree at most 2 in each variable,

$$W_h = \{v \in H^1(\Omega) : v|_E \in S_2(E) \ \forall E \in \mathcal{T}_h\} \quad (39)$$

where $S_2(E)$ denotes the space of serendipity polynomials of degree 2,

$$\Sigma_h = \{\sigma : \sigma|_E \in \Sigma_x \times \Sigma_y \ \forall E \in \mathcal{T}_h, \sigma \cdot \tau \text{ continuous at the interelement boundaries}\} \quad (40)$$

where τ is the tangential unit vector to each edge of each element E ,

$$\Sigma_x = Q_1(E) + \text{span}\{y^2\}$$

and

$$\Sigma_y = Q_1(E) + \text{span}\{x^2\}.$$

Assume, for the sake of simplicity, that Ω is a rectangle divided into rectangles E . The degrees of freedom for the spaces Θ_h and W_h on each element are the usual ones. We indicate by N_θ and N_W the dimension of the spaces Θ_h and W_h respectively. The

shape functions for the local space Σ_x are uniquely determined by the following five degrees of freedom:

$$\begin{aligned} & \int_E \sigma_x \, dx \, dy \\ & \int_e \sigma_x p_1(s) \, ds \quad \forall e \text{ horizontal edge of } E, \\ & \forall p_1(s) \text{ polynomial of degree } \leq 1 \text{ on } e \end{aligned} \quad (41)$$

Likewise, the five degrees of freedom for the local space Σ_y are the following:

$$\begin{aligned} & \int_E \sigma_y \, dx \, dy \\ & \int_e \sigma_y p_1(s) \, ds \quad \forall e \text{ vertical edge of } E, \\ & \forall p_1(s) \text{ polynomial of degree } \leq 1 \text{ on } e \end{aligned} \quad (42)$$

We indicate by $2N_\Sigma$ the dimension of the global space Σ_h . The degrees of freedom for the space Θ_h , W_h , Σ_x and Σ_y are indicated in Figure 2.

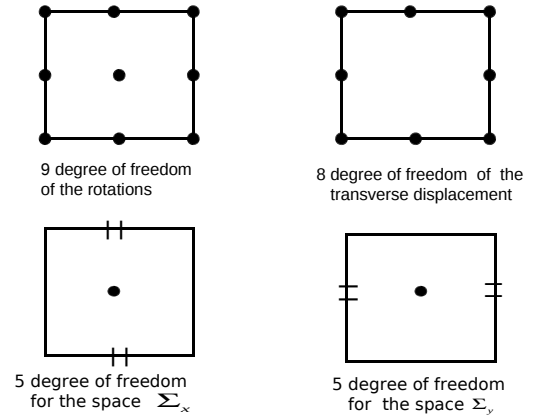


Figure 2: Degrees of freedom for the approximate spaces

Let $\{N^i\}_{i=1, \dots, N_\theta}$, $\{M^i\}_{i=1, \dots, N_W}$, $\{S_x^i, S_y^i\}_{i=1, \dots, N_\Sigma}$ be the basis functions for the spaces (38), (39), (40) respectively. The discrete solution of problem (29), $(\theta_x, \theta_y, w, \sigma_{xz}, \sigma_{yz})$,

can be written as:

$$\begin{aligned}\theta_x &= \sum_{i=1}^{N_\theta} (\theta_x)_i N^i, & \theta_y &= \sum_{i=1}^{N_\theta} (\theta_y)_i N^i, \\ w &= \sum_{i=1}^{N_W} w_i M^i, \\ \sigma_{xz} &= \sum_{i=1}^{N_\Sigma} (\sigma_x)_i S_x^i, & \sigma_{yz} &= \sum_{i=1}^{N_\Sigma} (\sigma_y)_i S_y^i\end{aligned}$$

Writing the corresponding problem in terms of degrees of freedom, we obtain as usual a linear system

$$\mathbf{K}\mathbf{U} = \mathbf{P}, \quad (43)$$

where \mathbf{U} represents the degrees of freedom of the discrete solution, \mathbf{P} the loading term and K the stiffness matrix.

We write the discretized form of the problem (29) in this way

$$\left\{ \begin{array}{ll} \text{Find } (\boldsymbol{\theta}, w, \boldsymbol{\sigma}) \in \boldsymbol{\Theta}_h \times W_h \times \boldsymbol{\Sigma}_h : \\ \frac{t^3}{12} a(\boldsymbol{\eta}, \boldsymbol{\theta}) + tk(\boldsymbol{\eta}, \boldsymbol{\sigma}) = 0 & \forall \boldsymbol{\eta} \in \boldsymbol{\Theta}_h \\ tk(\boldsymbol{\nabla} v, \boldsymbol{\sigma}) = t(v, p) & \forall v \in W_h \\ tk(\boldsymbol{\xi}, \boldsymbol{\theta}) + tk(\boldsymbol{\xi}, \boldsymbol{\nabla} w) - tk \frac{2(1+\nu)}{E} (\boldsymbol{\xi}, \boldsymbol{\sigma}) = 0 & \forall \boldsymbol{\xi} \in \boldsymbol{\Sigma}_h, \end{array} \right. \quad (44)$$

that in matricial form it becomes:

$$\begin{bmatrix} K_{11} & K_{12} & 0 & K_{14} & 0 \\ & K_{22} & 0 & 0 & K_{25} \\ & & 0 & K_{34} & K_{35} \\ \text{sym} & & & K_{44} & 0 \\ & & & & K_{55} \end{bmatrix} \mathbf{U} = \begin{bmatrix} 0 \\ 0 \\ \mathbf{P}_3 \\ 0 \\ 0 \end{bmatrix} \quad (45)$$

where

$$\begin{aligned}K_{11}(i, j) &= \frac{t^3}{12} a_{xx}(N^i, N^j), \quad i, j = 1, \dots, N_\theta \\ K_{12}(i, j) &= \frac{t^3}{12} a_{xy}(N^i, N^j), \quad i, j = 1, \dots, N_\theta \\ K_{14}(i, j) &= tk(N^i, S_x^j), \quad i = 1, \dots, N_\theta, \quad j = 1, \dots, N_\Sigma \\ K_{22}(i, j) &= \frac{t^3}{12} a_{yy}(N^i, N^j), \quad i, j = 1, \dots, N_\theta \\ K_{25}(i, j) &= tk(N^i, S_y^j), \quad i = 1, \dots, N_\theta, \quad j = 1, \dots, N_\Sigma \\ K_{34}(i, j) &= tk(M_x^i, S_x^j), \quad i = 1, \dots, N_W, \quad j = 1, \dots, N_\Sigma \\ K_{35}(i, j) &= tk(M_y^i, S_y^j), \quad i = 1, \dots, N_W, \quad j = 1, \dots, N_\Sigma \\ K_{44}(i, j) &= tk \frac{2(1+\nu)}{E} (S_x^i, S_x^j), \quad i, j = 1, \dots, N_\Sigma \\ K_{55}(i, j) &= tk \frac{2(1+\nu)}{E} (S_y^i, S_y^j), \quad i, j = 1, \dots, N_\Sigma \\ \mathbf{P}_3(i) &= t(p, M_i), \quad i = 1, \dots, N_W\end{aligned} \quad (46)$$

and $a_{rs}(\cdot, \cdot)$ represents the restriction of (30) to the corresponding fields θ_r and θ_s .

5.2. MITC multilayered plate element: FSDT and EM1-2 models

The application of the First Order Shear Deformation Theory to the multilayered plates in the RMVT context consists in an equivalent single layer description both of the displacement fields and the transverse stresses. Layer by layer a problem like to (29) has to be solved and this leads to a linear distribution of the displacement fields and a constant piecewise distribution of the transverse shear stresses along the thickness. Correspondingly the approximation of the multilayered plate problem following FSDT approach is achieved layer by layer. Using the MITC finite element this corresponds to solve layer by layer a problem like (44).

The approximation of the multilayered plate problem following the EM1-2 model in the RMVT context is obtained by discretizing layer by layer problem (36) and by linking the transverse stresses with the interlaminar transverse stress continuity (34) condition. In order to approximate problem (36) with MITC finite element we use the space $\boldsymbol{\Theta}_h$, (38), and W_h , (39), for the rotations and vertical displacement and we approximate each component

of the shear stress tensor $\tilde{\sigma} = [\sigma_t, \sigma_b, \sigma_2]$ with the space Σ_h , (40). This implies an approximation of $\tilde{\sigma}$ in the space Σ_h^3 .

6. Numerical results

The strategy we have introduced to solve the multilayered plate problem in the RMVT formulation provides an advanced locking-free finite element assuming the transverse stresses as independent variables. The method similar to MITC approach is based on a carefully choice of the finite element spaces for displacements and stresses. In order to present the performance of our element we test it on benchmark problems and we show that it exhibits good properties of convergence and robustness. We consider a plate model problem whose exact solution is known to analyze the convergence properties of the method and after we treat a benchmark sandwich plate to study the assessment of the MITC technique in the cases of multilayered plates.

6.1. Plate model problem

We present the numerical results concerning a unit clamped square plate $[0, 1] \times [0, 1]$ made of isotropic material whose the elastic constants are: $E = 3.D + 6 GPa$, $\nu = 0.3$. We analyze the behaviour of the plate versus the thickness t to show the robustness of the element with respect to the locking phenomenon. We take the value $t = 0.1$, $t = 0.01$, $t = 0.001$ corresponding to the case of thick to very thin plate. We deal with the vertical load:

$$p(x, y) = \frac{Et^2}{12(1-\nu^2)} [12y(y-1)(5x^2-5x+1)(2y^2(y-1)^2 + x(x-1)(5y^2-5y+1)) + 12x(x-1)(5y^2-5y+1)(2x^2(x-1)^2 + y(y-1)(5x^2-5x+1))], \quad (47)$$

that allows us to write the exact solution of this model problem in terms of rotations, vertical dis-

placement and shear strains as follows:

$$\begin{aligned} \theta_x(x, y) &= y^3(y-1)^3x^2(x-1)^2(2x-1) \\ \theta_y(x, y) &= x^3(x-1)^3y^2(y-1)^2(2y-1) \\ w(x, y) &= \frac{1}{3}x^3(x-1)^3y^3(y-1)^3 - \\ &\quad \frac{2t^2}{6k(1-\nu)} [y^3(y-1)^3x(x-1)(5x^2-5x+1) + \\ &\quad x^3(x-1)^3y(y-1)(5y^2-5y+1)] \\ \gamma_{xz}(x, y) &= -\frac{2t^2}{6k(1-\nu)} [y^2(y-1)^2(10x^2-10x+1) + \\ &\quad 3x^2(x-1)^2(5y^2-5y+1)](2x-1)y(y-1) \\ \gamma_{yz}(x, y) &= -\frac{2t^2}{6k(1-\nu)} [x^2(x-1)^2(10y^2-10y+1) + \\ &\quad 3y^2(y-1)^2(5x^2-5x+1)](2y-1)x(x-1) \end{aligned} \quad (48)$$

The exact transverse displacement and the shear strains on a quarter of the plate are shown in Figure 3, 4, 5.

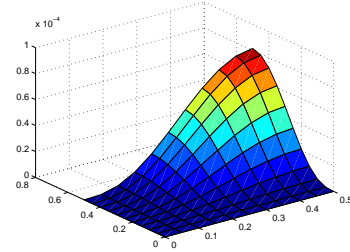


Figure 3: Transverse displacement w of model problem

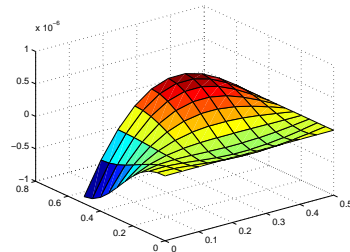


Figure 4: Shear strain γ_{xz} of model problem

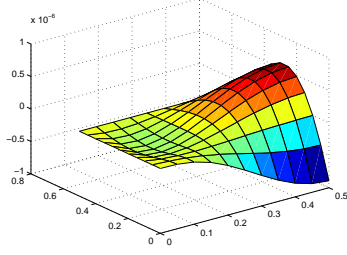


Figure 5: Shear strain γ_{yz} of model problem

We note that in the case of isotropic material the transverse shear strains and stresses are related by $\boldsymbol{\sigma} = G\boldsymbol{\gamma}$, with $G = \frac{E}{2(1+\nu)}$. Then from the knowledge of the strains it is easy to go back to the shear stresses. The model problem we have considered enables us to evaluate the relative errors between the exact and approximate solutions. In particular for the shear strains we analyze the relative error in L^2 -discrete norm:

$$(E_\gamma)^2 = \frac{\sum_{i=1}^{Ne} (\gamma(x_i, y_i) - \gamma_h(x_i, y_i))^2}{\sum_{i=1}^{Ne} (\gamma(x_i, y_i))^2} \quad (49)$$

where $\gamma_h(x, y) \in \Sigma_h$ is the finite element approximation of $\gamma(x, y)$, (x_i, y_i) are the coordinates of the barycenter of the i -th element of \mathcal{T}_h and Ne is the number of its elements. The Figures 6, 7, 8 represent the errors (49) for the case $t = 0.1 \div 0.0001$ respectively and exhibit the good properties of convergence of the method, even if the plate is very thin ($t = 0.0001$). The results show a numerically calculated second convergence rate according to the theoretical result ([30]). The robustness of the fi-

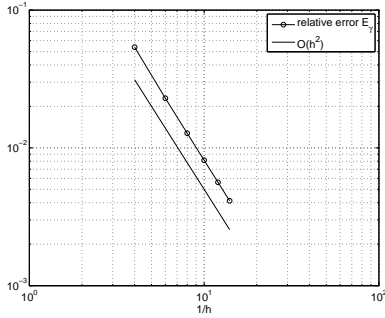


Figure 6: Shear strain error for the thickness $t = 0.1$

nite element with respect to the shear locking phenomenon is also confirmed in Figure 9. The transverse displacement corresponding to fixed values of

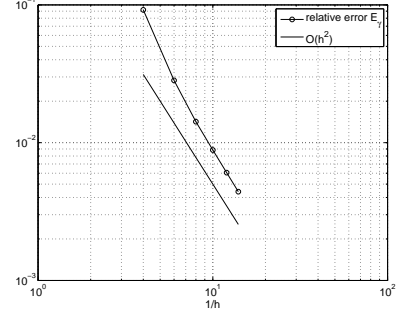


Figure 7: Shear strain error for the thickness $t = 0.01$

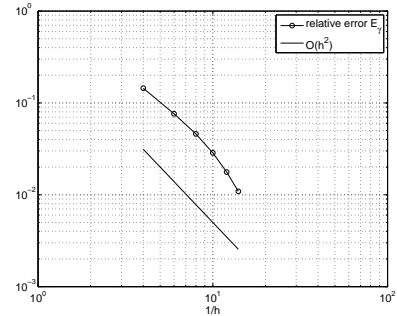


Figure 8: Shear strain error for the thickness $t = 0.001$

the discretization parameter h is depicted versus the (opposite of the logarithm of the) thickness of the plate and one can observe that the behaviour of the displacement does not deteriorate for all thicknesses of practical interest.

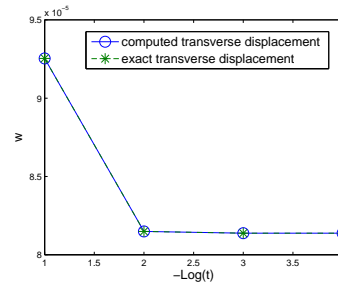


Figure 9: Transverse displacement versus the thickness

6.2. Sandwich plate

We have considered a benchmark test of a sandwich plate with isotropic core and skins (see [40])

Table 1: Elastic and geometrical properties of skins

Properties	Skins
E_s (GPa)	50
ν	0.25
G_s (GPa)	20
t_s (m)	0.1
$b=3a$	3,30,300

Table 2: Elastic and geometrical properties of core

Properties	Core
E_c (GPa)	1
ν	0.25
G_c (GPa)	0.4
t_c (m)	0.8
$b=3a$	3,30,300

as shown in Figure 10. The sandwich plate is simply supported and it is loaded with a bisinusoidal distribution of transverse pressure applied to the top plate surface:

$$p(x, y) = \sin\left(\frac{\pi x}{a}\right) \sin\left(\frac{\pi y}{b}\right)$$

The elastic and geometrical properties are reported

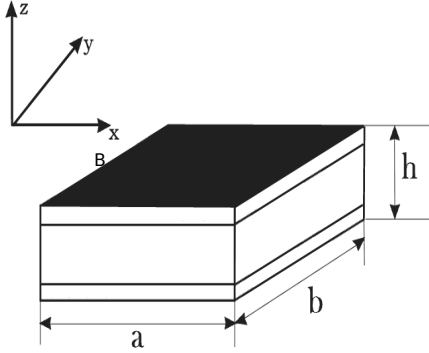


Figure 10: Sandwich plate

in Table 1, 2. We compare the results obtained with our Equivalent Single Layer Mixed method (EM1-2) with those obtained with the Layerwise Mixed model of fourth order (LM4) that can be

used (see [40]) as a quasi-3D solution for those cases in which complete 3D results are not available. Furthermore to validate the improvement of the behaviour of the solution approximated by EM1-2 model with respect to the FSDT approach described in subsection 5.2, we present also the comparison with this model. Due to the symmetry of the problem the stresses σ_{xz} and σ_{yz} behave in the same way and thus we analyze only the shear stress σ_{xz} . In Figures 11, 12, 13 we report the shear stress σ_{xz} of the sandwich plate evaluated at the middle point of plate-edge parallel to y -axis, for $a/t = 1 \div 100$, in the thickness direction. It is evident the quadratic approximation of the shear stresses by EM1-2 model compared with the piecewise constant approximation of FSDT model. One can note also that EM1-2 permits to satisfy the interlaminar continuity conditions, according to LM4 solution. In Figure 14 we emphasize what happens in the core. In Figures 15, 16 we plot the normalized transverse displacement \bar{w} of the sandwich plate:

$$\bar{w} = w \frac{100E_c}{t\left(\frac{a}{t}\right)^4}$$

As expected the FSDT and EM1-2 approaches give the same results, while the LM4 behaves differently in the case of the thick plate and similarly in the case of the thin plate. Anyway, by observing the figures, one can deduce that the modelling of shear stresses in EM1-2 model improves also the description of transversal displacement that slightly moves toward LM4 solution. The Figure 18 shows that the EM1-2 approach leads to a locking-free finite element to treat the multilayered plates. The normalized transverse displacement depicted in this figure confirms the performance and the robustness of the element even for very thin sandwich plate.

7. Conclusions

In this work an advanced locking-free finite element (EM1-2) for the analysis of the multilayered plates has been presented. The problem is modeled by adopting the variational formulation based on RMVT. A mixed theory with equivalent single layer (ESL) descriptions for the displacements and a layerwise (LW) description for the transverse stresses is considered. In particular a first order displacements field in conjunction with a parabolic transverse stresses field independent in each layer is adopted. The continuity condition of the transverse stresses at the interfaces between layers (IC)

is easily imposed by assuming the stresses as independent variables. The in-layer approximation is performed by a strategy similar to MITC (Mixed Interpolated Tensorial Components) finite element approach. A benchmark test of a sandwich simply supported plate with isotropic core and skins is considered to validate both properties of convergence and robustness of the element EM1-2 with respect to the 3D solutions. The comparison of the EM1-2 results with respect to the piecewise constant FSDT approximations shows an improvement of the behaviour of the solution as regards both the description of transverse displacement and the shear stresses. The analysis of the solution performed versus the thickness of the structure confirms that EM1-2 is a locking-free finite element able to treat the multilayered plates even for very thin structures.

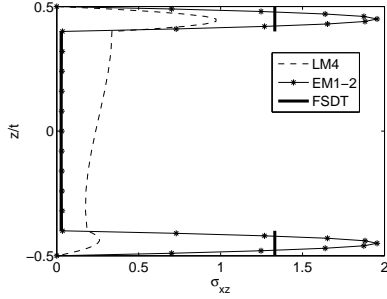


Figure 11: Shear stress σ_{xz} of the sandwich plate for $a/t=1$

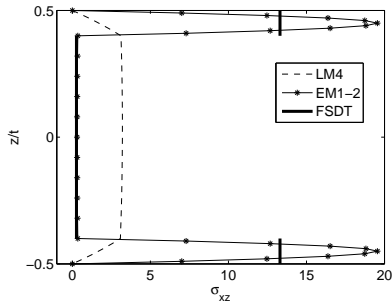


Figure 12: Shear stress σ_{xz} of the sandwich plate for $a/t=10$

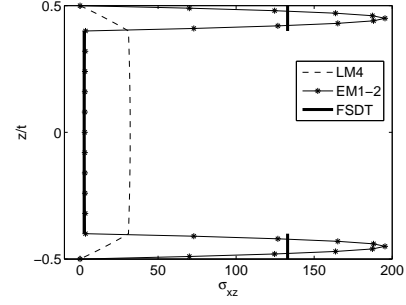


Figure 13: Shear stress σ_{xz} of the sandwich plate for $a/t=100$

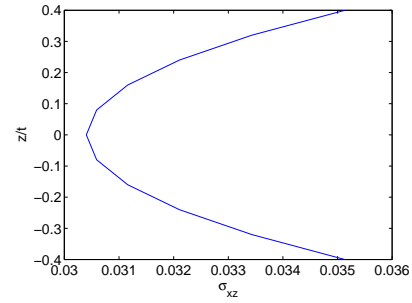


Figure 14: Shear stress σ_{xz} (EM1-2 element) in the core of the sandwich plate for $a/t=1$

References

- [1] Whitney J.M. The effects of transverse shear deformation on the bending of laminated plates. *J Compos Mat* 1969;3:534-547.
- [2] Pagano N. J. Exact solutions for Composite Laminates in Cylindrical Bending. *J Compos Mat* 1969;3:398-411.
- [3] Reissner E. On a certain mixed variational theory and a proposed application. *Int J Numer Methods Eng* 1984;20:13661368.
- [4] Reissner E. On a mixed variational theorem and on a shear deformable plate theory. *Int J Numer Methods Eng* 1986;23:193198.
- [5] Reissner E. On a certain mixed variational theorem and on a laminated elastic shell theory. *Proc of Euromech-Colloquium* 1986;219:1727.
- [6] Carrera E. Developments, ideas, and evaluations based upon Reissners Mixed Variational Theorem in the modeling of multilayered plates and shells. *Appl Mech Rev* 2001;54(4):301329.
- [7] Murakami H. Laminated composite plate theory with improved in-plane responses. *ASME Proc of PVP Conf, New Orleans* 1985;98-2:257263.
- [8] Murakami H. Laminated composite plate theory with improved in-plane responses. *ASME J Appl Mech* 1986;53:661666.
- [9] Toledano A., Murakami H. A high-order laminated plate theory with improved in-plane responses. *Int J Solids Struct* 1987;23:111131.

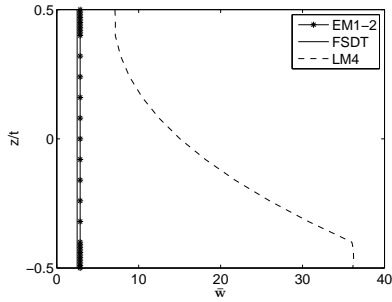


Figure 15: Normalized transverse displacement \bar{w} of the sandwich plate for $a/t=1$

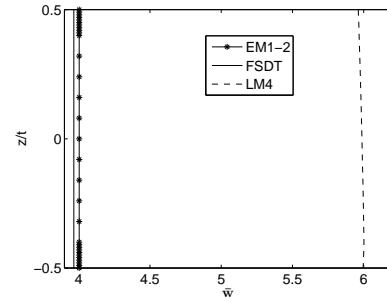


Figure 17: Normalized transverse displacement \bar{w} of the sandwich plate for $a/t=10$

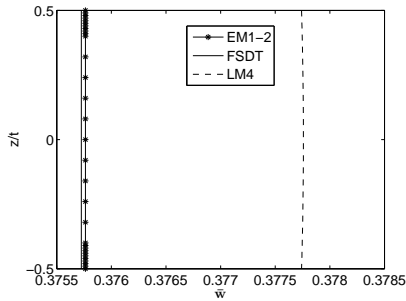


Figure 16: Normalized transverse displacement \bar{w} of the sandwich plate for $a/t=100$

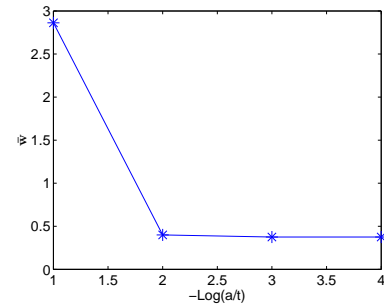


Figure 18: Normalized transverse displacement \bar{w} of the sandwich plate versus the thickness

- [10] Toledano A., Murakami H. A composite plate theory for arbitrary laminate configurations. ASME J Appl Mech 1987;54:181189.
- [11] Soldatos K.P. Cylindrical bending of cross-ply laminated plates: refined 2D plate theories in comparison with the exact 3D elasticity solution. Tech Report 140, Dept. of Math., University of Ioannina, Greece.
- [12] Carrera E. A class of two-dimensional theories for anisotropic multilayered plates analysis. Accademia delle Scienze di Torino, Memorie Scienze Fisiche 1995;19-20:139.
- [13] Carrera E. C_0^z Requirements-models for the two dimensional analysis of multilayered structures. Compos Struct 1997;37:373384.
- [14] Carrera E. Recent Developments in the Modeling of Multilayered Plates and Shells based upon Reissner's Mixed Equation. In: XIV congresso AIMETA, Como 6-9 October 1999.
- [15] Carrera E. A Reissner's mixed variational theorem applied to vibration analysis of multilayered shells. ASME J Appl Mech Como 1999;66:6978.
- [16] Carrera E. Mixed layer-wise models for multilayered plates analysis. Compos Struct 1998;43:5770.
- [17] Carrera E. Evaluation of layer-wise mixed theories for laminated plates analysis. AIAA J 1998;26:830839.
- [18] Carrera E. Transverse normal stress effects in multilayered plates. ASME J Appl Mech 1999;66:10041012.
- [19] Carrera E. A study of transverse normal stress effects on vibration of multilayered plates and shells. J Sound Vib 1999;225:803-829.
- [20] Carrera E. Single-layer vs multi-layers plate modellings on the basis of Reissner's mixed theorem. AIAA J 2000;38(2):342352.
- [21] Carrera E. A priori vs a posteriori evaluation of transverse stresses in multilayered orthotropic plates. Compos Struct 2000;48:245-260.
- [22] Carrera E. Vibrations of layered plates and shells via Reissner's Mixed Variational Theorem. In: Fourth Symposium on Vibrations of Continuous Systems, Kensington, 2003, July 7-11, 4-6.
- [23] Carrera E. Layer-wise mixed models for accurate vibration analysis of multilayered plates. ASME J Appl Mech 1998;65:820828.
- [24] Messina A. Two generalized higher order theories in free vibration studies of multilayered plates. J Sound Vib 2001;242:125150.
- [25] Carrera E., Demasi L. Sandwich plates analyses by finite element method and Reissner's Mixed Theorem. In: Sandwich V, Zurich, 2000, September 5-7, 301-313.
- [26] Carrera E., Demasi L. Multilayered finite plate element based on Reissner Mixed Variational Theorem. Part I: Theory. Int J Numer Meth Eng 2002;55:191-231.
- [27] Carrera E., Demasi L. Multilayered finite plate element based on Reissner Mixed Variational Theorem. Part II: Numerical Analysis. Int J Numer Meth Eng 2002;55:253-296.

- [28] Zienkiewicz O.C., Taylor R.L., Too J.M. Reduced integration techniques in general analysis of plates and shells. *Int J Numer Meth Eng* 1971;3:275-290.
- [29] Huang H.-C. Membrane locking and assumed strain shell elements. *Comput Struct* 1987;27(5):671-677.
- [30] Brezzi F., Bathe K.-J., Fortin M. Mixed-interpolated elements for Reissner-Mindlin plates. *Int J Numer Meth Eng* 1989;28:1787-1801.
- [31] Chinosi C., Della Croce L. Mixed-interpolated elements for thin shell. *Commun Numer Meth Eng* 1998;14:1155-1170.
- [32] Bathe K.-J., Lee P.-S., Hiller J.-F. Towards improving the MITC9 shell element. *Comput Struct* 2003;81:477-489.
- [33] Panasz P., Wisniewski K. Nine-node shell elements with 6 dofs/node based on two-level approximations. Part I Theory and linear tests. *Fin Elem Anal Design* 2008;44:784-796.
- [34] Cinefra M., Chinosi C., Della Croce L. MITC9 shell elements based on refined theories for the analysis of isotropic cylindrical structures. *Mech Adv Mater Struct*, DOI:10.1080/15376494.2011.581417.
- [35] Carrera E. Theories and finite elements for multilayered, anisotropic, composite plates and shells. *Arch Comput Meth Engng* 2002;9(2):87-140.
- [36] Reissner E. The effect of transverse shear deformation on the bending of elastic plates. *ASME J Appl Mech* 1945;12:69-76.
- [37] Mindlin R.D. Influence of rotatory inertia and shear in flexural motions of isotropic elastic plates. *ASME J Appl Mech* 1951;18:1031-1036.
- [38] Bathe K.-J., Dvorkin E.N. A formulation of general shell elements - The use of Mixed Interpolation of Tensorial Components. *Int J Numer Meth Engng* 1986;22:697-722.
- [39] Bathe K.-J., Brezzi F., Cho W. The MITC7 and MITC9 plate bending elements. *Comput Struct* 1989;32:797-841.
- [40] Carrera E., Brischetto S. A survey with numerical assessment of classical and refined theories for the analysis of sandwich plates. *Appl Mech Rev* 2009;62(1):010803(17 pages).